Proceedings of the 20th International Conference on Soil Mechanics and Geotechnical Engineering– Rahman and Jaksa (Eds)

Assessment of liquefaction triggering potential of Sabkha soils in the U.A.E. and development of probabilistic ground motion estimates

Évaluation du potentiel de liquéfaction des Sabkha sols aux E.A.U. et développement d'estimations probabilistes des mouvements du sol

Chulmin Jung & Eungu Kang
Samsung Engineering, Seoul, South Korea, chulmin.jung@samsung.com

Amalia Giannakou & Jacob Chacko
GR8 GEO, Athens, Greece, agiannakou@gr8-geo.com

ABSTRACT: This paper presents a case study for the assessment of liquefaction triggering potential of Sabkha soils encountered at an oil & gas project site in Ruwais, U.A.E. A comprehensive geotechnical investigation that included field tests such as SPT, CPT and in-situ shear wave velocity measurements was performed to characterize the subsurface conditions at the site. 1D site response analysis was performed to develop seismic demand estimates for use in liquefaction triggering assessments using bedrock g round motion levels defined in the Abu Dhabi International Building Code (ADIBC 2013). Three different simplified liquefaction triggering evaluation methods were used to evaluate the liquefaction triggering potential of the Sabkha soils. Evaluations using SPT and CPT tests to assess the liquefaction triggering resistance of the Sabkha soils yielded similar results indicating factors of safety against liquefaction varying from 1.2 to more than 1.5. In addition, site-specific PSHA were performed to develop reliable estimates of the hazard at the site for bedrock conditions and comparisons are made with ADIBC (2013) and other regional studies.

RÉSUMÉ : Cet article présente un cas pour l'évaluation du potentiel de liquéfaction des Sabkha sols qui ont été rencontrés sur un projet de pétrole et gaz à Ruwais, E.A.U. Une étude géotechnique avec des tests sur site comme SPT, CPT et des mesures in situ de la vitesse des ondes de cisaillement a été réalisée pour caractériser les conditions souterraines dans le site. 1D analyse de la réponse du site a été réalisée pour développer des estimations de la demande sismique à utiliser dans les évaluations de liquéfaction en utilisant les niveaux de mouvement du substratum rocheux définis dans le Abu Dhabi International Building Code (ADIBC 2013). Trois différentes méthodes simplifiées d'évaluation de la liquéfaction ont été utilisées pour évaluer le potentiel de la liquéfaction des Sabkha sols. Les évaluations utilisant des tests SPT et CPT pour évaluer la résistance à la liquéfaction des Sabkha sols ont présenté des résultats similaires indiquant des facteurs de sécurité contre la liquéfaction variant de 1.2 à plus de 1.5. Un plus, une PSHA spécifique du site a été réalisée pour développer des estimations du risque dans le site pour les conditions du substratum rocheux et des comparaisons sont réalisée avec ADIBC (2013) et d'autres études régionales.

KEYWORDS: Liquefaction, Sabkha soils, Site response analysis, PSHA, U.A.E. ground motions

1 BACKGROUND

The oil & gas project site is situated in Ruwais Industrial Area, 240 km west of Abu Dhabi City, United Arab Emirates (U.A.E.)

The soil conditions consist of about 6.5 m of dense to very dense sand, which is dredged reclaimed fill, overlying approximately 3-meters of Sabkha soils. Sabkha soils are coastal, supratidal sediments containing evaporite-saline minerals deposited in an arid climate and range from loose silty sands to soft clayey sands or silts. Assessing the liquefaction potential of Sabkha soils is a key geotechnical engineering issue associated with these types of deposits.

The design levels for the site were defined per the requirements of the Abu Dhabi International Building Code (ADIBC, 2013). A bedrock acceleration response spectrum applicable at about 15 m depth was developed for the Maximum Credible Earthquake (MCE) with 2475-year return period following the provisions in ADIBC (2013) and using the mapped spectral accelerations included in the code. Site response analyses were performed to develop estimates of seismic demand (i.e. Cyclic Stress Ratio) for use in liquefaction triggering evaluations. The cyclic resistance to liquefaction was estimated from available in situ tests (i.e. CPTs and SPT blowcounts) using NCEER (Youd et al., 1997), Idriss and Boulanger (2008) and Boulanger and Idriss (2014) empirical correlations for liquefaction triggering assessment.

In addition, site-specific Probabilistic Seismic Hazard Analyses (PSHA) were performed to develop reliable estimates of the hazard at the site for bedrock conditions and comparisons are made with ADIBC (2013) and other regional studies.

2 SOIL CONDITIONS AND SHEAR WAVE VELOCITY

Available geotechnical data included one borehole with SPT blowcounts, which is thought to be representative of the site, and associated basic laboratory tests, data from downhole shear wave velocity measurement and one CPT. An idealized profile was developed based on the subsurface conditions interpreted from the available geotechnical data.

Figure 1 plots SPT blowcounts, fines content measurements, CPT tip resistance q_c and soil behavior type index I_c with depth. The CPT plots are colour-coded based on Robertson (1990) soil classification with coarse-grained layers (i.e. I_c<2.6) shown in yellow and green and fine-grained layers (i.e. I_c>2.6) shown in pink and red. As shown on this figure, the primary units in descending sequence include:

- Dense coarse-grained fill extending from ground surface to about 1.5 m depth
- Dense to very dense silty sand extending from 1.5 m to about 6.5 m depth with SPT blowcounts varying from 50 to refusal and CPT tip resistances larger than 20 MPa
- Very loose silty sand (Sabkha) extending from 6.5 m to 9.5 m with SPT blowcounts varying from 0 to 1 and fines

content measurements varying from 25% to 35%. CPT data within this layer imply high fines content (i.e. high I_c values) and low tip resistance (i.e. about 2 MPa)

- Dense to very dense silty sand extending from 9.5 m to 15.5 m with blowcounts varying from 23 to refusal and CPT tip resistances of about 18 MPa
- Sandstone extending from 15.5 m to the maximum depth explored

It is noted that CPT data within the Sabkha layer shows interlayering of thin coarse-grained (yellow colours) and fine-grained (pink and red colours) material which may influence the maximum tip resistance that develops in the coarse-grained layers. This issue cannot possibly be picked up by the SPT blowcounts.

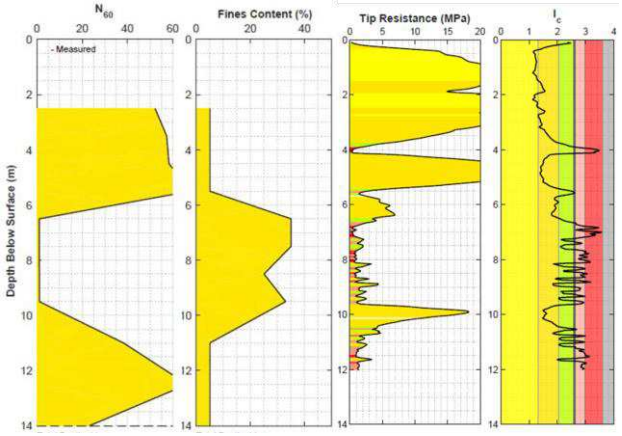

Figure 1. SPT blowcounts, fine content measurements, CPT tip resistance, and I_c factor colour-coded per Robertson (1990) soil classification.

An idealized shear wave velocity profile was developed for the site response analyses. Downhole seismic tests were performed in accordance with the requirements of ASTM D7400 and shear wave velocity measurements were obtained at 1 -m intervals. In addition to the downhole data that provide direct measurements of shear wave velocity versus depth, the average of empirical correlations between CPT tip resistance and shear wave velocity from Andrus (2017), Robertson (2009) and Mayne (2006) were used to develop shear wave velocity estimates from the available CPT data.

The measured and interpreted shear wave velocity profiles are plotted on Figure 2 versus depth together with the idealized profile (black line) used in the site response analyses. As shown on this figure a relatively large difference is observed between the downhole shear wave velocity measurement and the interpreted shear wave velocity from CPT data within the Sabkha deposit, with the measured velocities being almost double of the interpreted. As shown on Figure 2 the measured shear wave velocity values only slightly decrease within the Sabkha layer, dropping from about 260 m/s in the overlying dense sand to about 200-220 m/s in the Sabkha deposit. The downhole method measures average seismic velocities at various depths between the source at the surface and receiver within the borehole. Therefore, the presence of the relatively thick, dense sand layer near the ground surface seems to have influenced the velocity measurements within the underlying loose sand. To address the uncertainty related to the shear wave velocity of the Sabha deposit two shear wave velocity values., 100 m/s and 200 m/s, were considered for this unit in the site response analyses.

3 SITE RESPONSE ANALYSES

3.1 *Methodology*

Nonlinear site response analyses were performed with the computer code DEEPSOIL 6.1 (Hashash et al, 2015). DEEPSOIL is a one-dimensional site response analysis program that can perform both nonlinear and equivalent linear analyses.

The General Quadratic/Hyperbolic (GQ/H) model (Groholski et al, 2015) was used for the analyses because it provides the ability to represent small-strain stiffness nonlinearity as well as to define the shear strength. In this model the unload-reload stiffness uses a non-Masing criterion via inclusion of a damping reduction factor to match laboratory measured damping curves.

Since no site-specific dynamic laboratory tests are available for the site, Darendeli's (2001) modulus reduction and damping curves were used for the different sand layers with a plasticity index (PI) equal to 0.

Friction angles of 40 and 33 degrees were used for the dense sand and Sabkha layers, respectively.

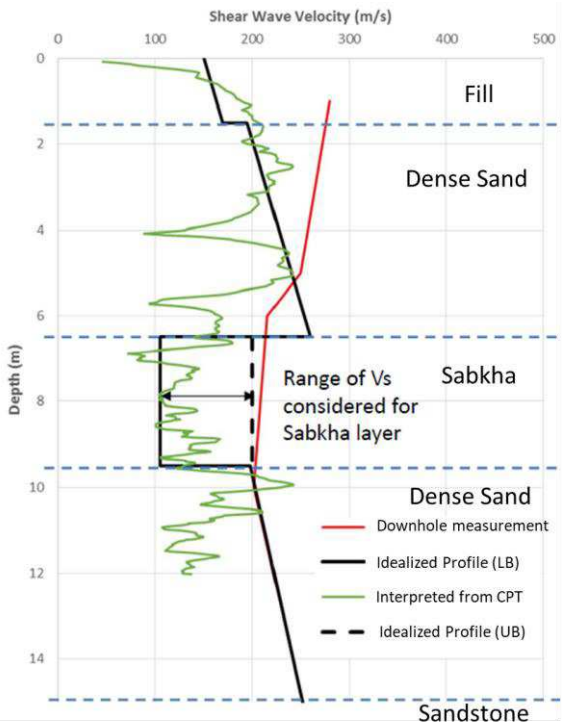

Figure 2. Measured and interpreted shear wave velocity and idealized Lower Bound (LB) and Upper Bound (UB) profiles considered in the site response analyses.

3.2 *Development of Input Time Histories*

Acceleration time histories at the bedrock horizon (V_{s30} = 370 m/s) were developed for use in site response analyses. Development of time histories generally included the following two steps:

1. Selection of seed time histories compatible with the target spectrum developed in accordance with ADIBC(2013) for a Maximum Credible Earthquake (MCE) with a corresponding return period of 2475-years; and
2. Modification of the seed time histories to match the target spectra

A bedrock acceleration response spectrum representative at top of sandstone was developed in accordance with the provisions of ADIBC (2013) and ASCE 7-05. The mapped S_s and S_1 acceleration values from ADIBC (2013) are 0.45 and 0.13 for V_{s30}=760 m/s. The response spectra at the top of sandstone with

a V_{s30} of 370 m/s were developed by applying code-based site amplification factors (F_a=1.2 and F_v=1.67) for Site Class C.

Seven sets of time histories (2 horizontal components) were selected and spectrally matched to the target bedrock spectrum. The seed acceleration time histories were modified by adding wavelets in the time domain to obtain response spectra compatible with the target spectra. The time-domain spectral matching was accomplished using the computer code RSPMATCH (Abrahamson 2003). Figure 3 presents example time histories of acceleration, velocity, and displacement as well as 5%-damped acceleration response spectra of one scaled (to the PGA of the target spectrum) seed, and spectrally modified motion.

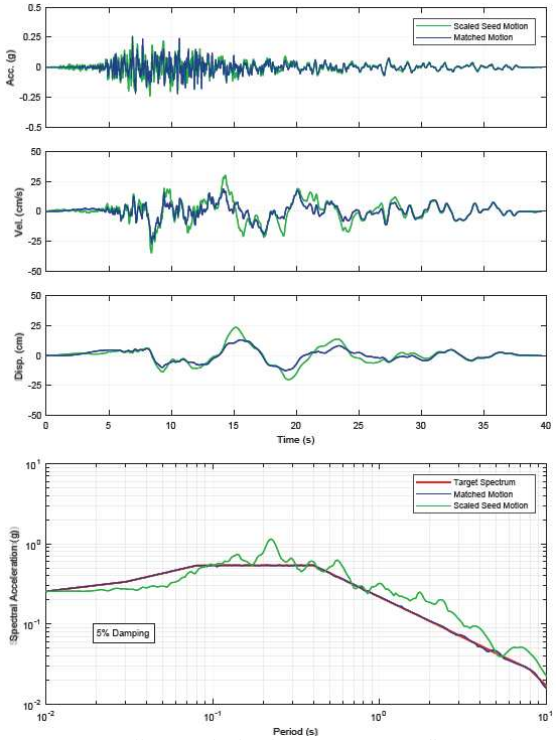

Figure 3. Spectrally matched El Centro Array #13 Motion, 140 Component, 1979 Imperial Valley Earthquake, USA, MCE level

3.3 *Results*

Site response analyses were performed for the 7 sets of matched time histories to the MCE spectrum at bedrock level and 2 shear wave velocity values for the Sabkha layer (i.e. lower bound and upper bound).

Figure 4 presents distributions with depth of maximum acceleration, maximum shear strain and cyclic stress ratio (CSR) for the lower bound (green line) and upper bound (red line) shear wave velocity of the Sabkha layer. The results shows on Figure 4 represent the mean response of the 14 ground motions considered in the site response analyses. The CSR was estimated as 65% of the maximum shear stress divided by the in situ vertical effective stress. As shown on this figure, the lower bound shear wave velocity profile results in larger strains within the Sabkha deposit and lower CSRs and PGA at the ground surface compared with the upper bound profile. The CSRs from the lower bound velocity profile of the Sabkha layer were used in the liquefaction triggering assessment described below as they were considered to be more realistic.

4 LIQUEFACTION TRIGGERING ASSESSMENT

Liquefaction triggering evaluations were performed to assess the liquefaction triggering potential of the loose Sabkha deposits. The liquefaction triggering evaluations were based on:

- CSR estimated directly from total-stress non-linear site-specific response analyses for MCE level event;
- A earthquake with magnitude M_w of 5.5
- Cyclic resistance of the Sabkha deposit evaluated from SPT blowcounts and cone penetration test (CPT) tip resistance data using three methods: NCEER (Youd et al., 1997), Idriss and Boulanger (2008) and Boulanger and Idriss (2014).

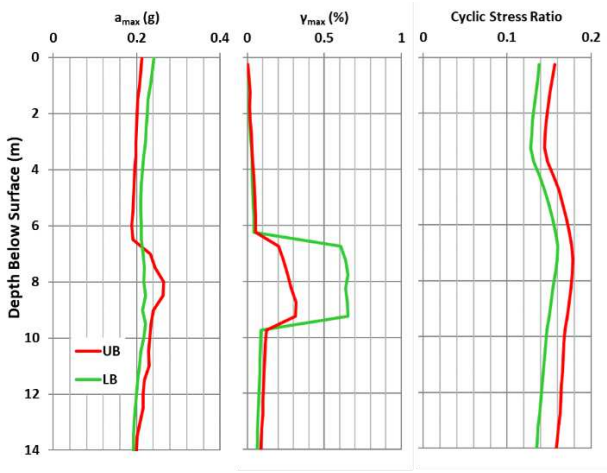

Figure 4. Profiles of maximum acceleration, maximum shear strain and cyclic stress ratio for Upper Bound and Lower Bound profiles (mean of all motions)

Figure 5 presents the results of the liquefaction triggering assessment based on SPT and CPT data using Idriss and Boulanger (2008) method. The first two plots from the left show the measured SPT blowcounts and the estimated factor of safety against liquefaction based on SPT data. The third plot presents the measured CPT tip resistance and the tip resistance that would be required to produce a factor of safety against liquefaction of 1. Areas where the former is less than the latter are shaded in blue. The last plot shows the estimated factor of safety against liquefaction from CPT data (black dots) and the I_c factor (red line).

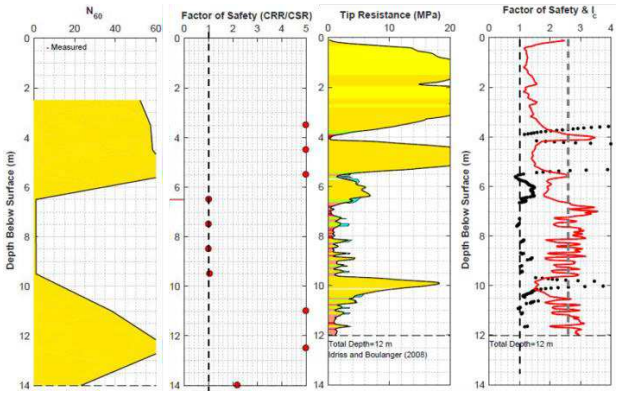

Figure 5. Liquefaction triggering evaluation results based on SPT blowcounts (first and second plot from the left) and CPT tip resistance (third and fourth plot from the left)

Liquefaction triggering evaluations from CPT data give a more detailed assessment within the Sabkha layer indicating factor of safety against liquefaction varying between 1.2 and more than 1.5 due to the interlayering of thin coarse- and fine-grained layers within the deposit, and are reflective of the fact that factors of safety close to 1 only occur within a very limited thickness within the Sabkha layer where the tip resistance drops likely due to the presence of very thin fine-grained interlayers (of

less than about 0.2 m thickness). As noted above the interlayering of thin coarse-grained (yellow colours) and fine-grained (pink and red colours) material that is observed from the CPT data in the Sabkha deposit may influence the maximum tip resistance that develops in the coarse-grained layers within the deposit leading to an underestimation of cyclic resistance. On the contrary the assessment from SPT blowcounts seems to imply a factor of safety of about 1 for the entire Sabkha layer since the influence of thin fine-grained interlayers cannot be captured with this method.

This is also shown on Figure 6 that presents a comparison of the interpreted fines content within the Sabkha layer estimated from CPT data using the three empirical correlations considered and lab measurements of fines content. As shown on this figure CPT interpreted data provide a continuous picture of the variation of fines within the Sabkha layer that implies the presence of fine-grained layers of limited thickness. On the other hand, lab measurements of fines content only provide estimates at every meter within the layer and a measurements of fines content from a disturbed sample that may include mixtures of coarse and fine grained thin layers.

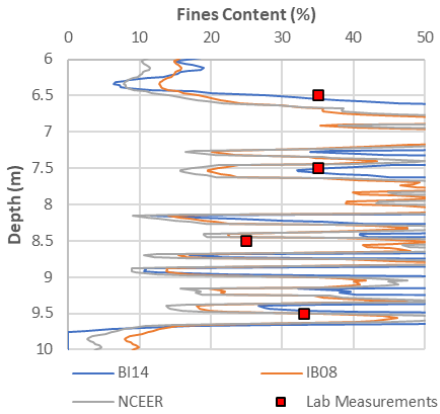

Figure 6. Measured and interpreted fines content from CPT data.

5 SITE-SPECIFIC GROUND MOTION DEVELOPMENT

Site specific PSHA were performed to develop acceleration resp onse spectra for shear wave velocities, V_{s30}, of 760 m/s (Site Cl ass B/C boundary) and 370 m/s.

5.1 *Seismic Source Model*

A project-specific seismic source model was developed to assess ground motion hazard at the site (Figure 7). The model includes two different types of sources: a) line sources representing well-characterized active faults and b) areal source zones representing the potential for earthquakes from unidentified, shallow crustal sources and deep subduction intraplate sources within approximately 300 km from the site. Information regarding the geological, tectonic and seismological setting derived from peer-reviewed literature, previously published seismotectonic models and earthquake catalogs (e.g., Abdalla and Al-Homoud, 2004; AI-Haddad et al., 1994; Al-Homoud, 2005; Jamali et al., 2006; Shabani and Mirzaei, 2007; Tavakoli and Ghafory-Ashtiany, 2004; Thenhaus et al.,1989; Wyss and Al-Homoud, 2004) was used to develop the seismic source model for the site. The major tectonic elements that could impact the project seismic hazard include:

- Arabian Platform Transition (represented by Areal Source Zone 1 on Figure 7),
- Mesopotamian Basin (represented by Areal Source Zone 2 on Figure 7),
- Oman Peninsula (represented by Areal Source Zone 8 and associated faults 4 to 6 on Figure 7),
- Zagros collision zone (represented by Areal Source Zones 3 to 7 and associated faults 1 to 3 and 7 on Figure 7) and
- Makran subduction zone (represented by Areal Source Zones 11 and 12 and interface line source 8 and Areal Source Zone 10 on Figure 7)

The activity of the shallow crustal areal source zones and the subduction intraplate sources was modeled by fitting a Gutenberg-Richter truncated exponential curve to the historical seismicity data. The activity of the fault sources is modeled by means of the fault slip rate in conjunction with the pure characteristic magnitude model. This is intended to model the large magnitude, characteristic-type events generated on these faults. The activity for the subduction interface source was modeled using the Youngs and Coppersmith (1985) characteristic model along with seismogenic slip rates.

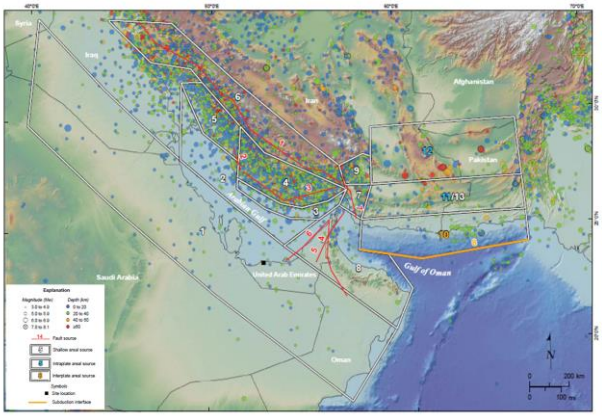

Figure 7. Seismic source model and historic seismicity.

A composite seismicity catalog over the region of the Arabian Gulf was compiled for the project. After compiling a combined catalog from multiple agencies and sources, events less than magnitude 3.0, and duplicate events were removed based on similarities in time, location, and magnitude. The raw undeclustered catalog was declustered using the Gardner-Knopoff time-space windows. The undeclustered seismicity is plotted on Figure 7. An evaluation of catalog completeness for different magnitudes was conducted to develop annual magnitude recurrence plots presented below.

5.2 *Probabilistic Seismic Hazard Analyses*

Probabilistic Seismic Hazard Analyses (PSHA) were carried out using the computer program HAZ43 (Abrahamson, 2013). HAZ43 was developed by Dr. Abrahamson and has been validated in the PSHA Validation Project performed by the Pacific Earthquake Engineering Research (PEER) Center's Lifelines Program (Thomas et al., 2010).

Epistemic uncertainty was accounted for through a logic tree approach with respect to the following modelling assumptions and parameters:

- Ground motion prediction equation (GMPE). Five GMPEs with equal weights were used to model the shallow crustal sources [i.e. Abrahamson et al. (2014), Boore et al. (2014), Campbell and Bozorgnia (2014), Chiou and Youngs (2014) and Akkar et al. (2014)] that are characterized as Active Crustal Regions such as the Zagros collision zone and the Oman Peninsula. Five GMPEs with equal weights [i.e. Atkinson (2008, 2011), Atkinson and Boore (2006, 2011), Pezeshk et al (2011), Silva et al (2002) and Toro et al (1997)] were used to model the shallow crustal areal sources that are characterized as Stable Continental Regions (SCR) such as the Arabian Platform Transition. Three GMPEs with

equal weights were used to model the Makran subduction sources [i.e. BC Hydro (Abrahamson et al., 2016), Zhao et al (2006) and Atkinson and Boore (2003, 2008)].

- Maximum/characteristic earthquake magnitude on the areal and planar fault sources. Three different maximum or characteristic magnitudes were considered for each zone.
- Slip rate on the planar fault sources and inter-plate subduction zone. Three different slip rates were considered for the planar fault sources and the inter-plate subduction zone.
- Dip angle of the planar fault sources. Typically, three different dip angles were considered for the planar fault sources.
- Style of faulting of the areal sources. Up to two styles of faulting were considered for the areal sources;
- Seismogenic depth of the shallow crustal areal sources. Two or three different seismogenic depths were considered for the shallow crustal areal sources

Uniform Hazard Spectra (UHS) were estimated for a return period of 2475 years in order to develop the Maximum Considered Earthquake Spectra per ADIBC (2013) for shear wave velocities of 760 m/s and 370 m/s. The ADIBC (2013) has adopted the 2009 version of the International Building Code (IBC) for the Abu Dhabi region. PSHA were conducted to develop design ground motion criteria for the Maximum Considered Earthquake (MCE) as defined by ASCE 7-05 (ASCE, 2006).

Figure 8 presents the uniform hazard spectra for V_{s30} values of 760 m/s and 370 m/s together with the S_s and S_1 mapped values from ADIBC (2013). The S_S and S_1 values from the site-specific PSHA were estimated to be 0.161 and 0.058, respectively, which are significantly lower than the mapped values of S_s=0.45 and S_1=0.13 provided in ADIBC (2013). Also shown on this figure (right plot) is a comparison of the site amplification factors estimated from the PSHA for V_{s30} 760 m/s and 370 m/s and the code-based site amplification factors (i.e. F_a and F_v). As shown the GMPE-based amplification factors are generally higher than the code-based factors.

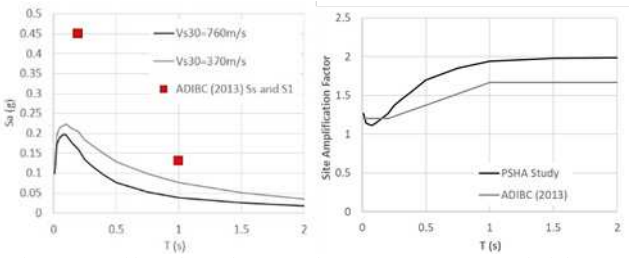

Figure 8. Uniform hazard spectra for 2475-year return period for V_{s30} values of 760 m/s and 370 m/s and site amplification factors estimated from the PSHA and ADIBC (2013)

Figure 9 shows a comparison of the PSHA MCE spectra for V_{s30} of 370 m/s and the MCE spectra estimated from ADIBC (2013) for Site Class C that were used as input in the site response analyses. As shown on this figure the PSHA MCE spectra are significantly lower than the code-based spectra due to the differences in the estimated seismic hazard at the site between the current study and ADIBC (2013).

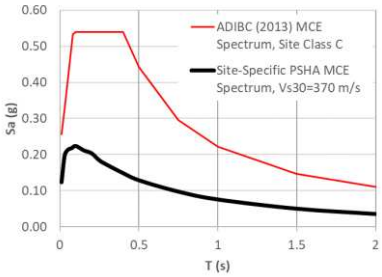

Figure 9. Comparison of the PSHA MCE spectra for V_{s30} of 370 m/s and the MCE spectra estimated from ADIBC (2013) for Site Class C

Figure 10 presents bar plots illustrating the fractional contribution to the total mean hazard from different seismic sources for 2475-year return period event and V_{S30} of 760 m/s. For short structural periods (i.e., PGA), the majority of the hazard, is associated with Areal Source zone A1 – Arabian Platform Transition which hosts the site. At longer structural periods (e.g., T = 1 s), the majority of hazard is driven by planar source F3 – Zagros Foredeep Fault South (located more than 200 km away from the site) and areal source zone A1 – Arabian Platform Transition which hosts the site.

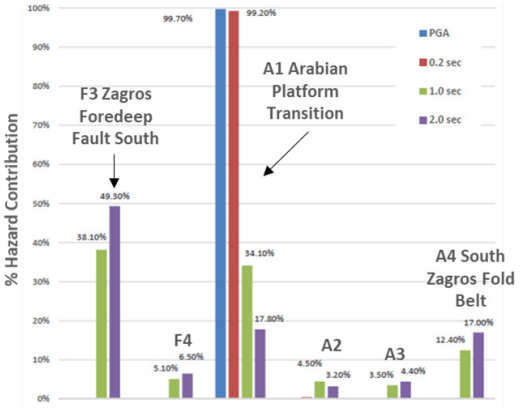

Figure 10. Hazard deaggregation by seismic source for 2475-year RP.

The results of the site-specific PSHA were also compared with the Global Seismic Hazard Assessment Program (GSHAP) map (Shedlock et al., 2000) which provides the 475-year return period PGA values per region for V_{s30} of 760 m/s. For the project area, GSHAP provides a PGA much lower than 0.01 g, which indicates very low hazard. The site-specific PSHA results give an estimated PGA of 0.032g for 475-years return period.

6 CONCLUSIONS

A liquefaction triggering assessment of Sabkha deposits encountered at a site in U.A.E. has been performed using ADIBC (2013) to develop ground motion estimates at bedrock level and site-specific response analyses to directly estimate cyclic stress ratio demand. Cyclic resistance was estimated using SPT and CPT data. It was found that liquefaction triggering evaluations from CPT data give a more detailed and reliable assessment within the Sabkha layer due to the interlayering of thin coarse- and fine-grained layers within the deposit compared to SPT blowcounts which seem to imply homogenous conditions for the entire Sabkha layer since the influence of thin fine-grained interlayers cannot be captured with this method.

In addition, a site-specific PSHA was performed to develop ground motion estimates for V_{s30} of 760 m/s (Site Class B/C boundary) and 370 m/s. It was found that the S_s and S_1 values estimated through the site-specific PSHA are significantly lower than ADIBC (2013) values and more in line with regional models (i.e. GEM) that imply a very low seismic hazard level at the site.

Considering the reduction in seismic demand due to the more reliable site-specific PSHA results a minimum FS against liquefaction of 1.2 is estimated (even when considering the minimum limits of 80% of the mapped values of S_s and S_1 from ADIBC2013) implying a low liquefaction risk of the Sabha soils for the specific site.

7 REFERENCES

Abrahamson N.A. 2003. RSPMATCH Software.

Abrahamson, N.A., 2013. HAZ43, Seismic Hazard Analysis Software.

Abrahamson N.A., Silva W.J. and Kamai R. 2014. Summary of the ASK14 ground motion relation for active crustal regions, *Earthquake Spectra* 30 (3), 1025-1055.

Abrahamson N.A., Gregor N. and Addo K. 2015. BC Hydro Ground Motion Prediction Equations for Subduction Earthquakes, *Earthquake Spectra*, 32 (1), 23-44.

Abdalla J.A. and Al-Homoud A.S. 2004. Seismic hazard assessment of United Arab Emirates and its surroundings, *Journal of Earthquake Engineering* 8 (6), 817-837.

Abu Dhabi International Building Code (ADIBC). 2013 Edition.

Akkar S., Sandikkaya M.A. and Bommer J.J. 2014. Empirical ground-motion models for point- and extended-source crustal earthquake scenarios in Europe and the Middle East, *Bulletin of Earthquake Engineering*, 12 (1), 359-387.

AI-Haddad M., Siddiqi G.H., AI-Zaid R., Arafah A., Necioglu A. and Turkelli N. 1994. A Basis for Evaluation of Seismic Hazard and Design Criteria for Saudi Arabia, *Earthquake Spectra* 10 (2), 231-258.

Al-Homoud A. 2005. Earthquake Hazard Analysis and Dynamic Site Response Evaluation for Design of Tower Buildings in Dubai, UAE, *76th Shock & Vibration Symposium: Destin*, FL, Shock and Vibration Information Analysis Center, p. 4-5.

American Society of Civil Engineers. 2006. *ASCE Standard 7-05 – Minimum Design Loads for Buildings and Other Structures*, ASCE 7-05.

Andrus R.D., Mohanan N.P., Piratheepan P., Ellis B.S. and Holzer T.L. 2007. Predicting shear-wave velocity from cone penetration resistance, *Proc., 4th Inter. Conf. on Earthq. Geotech. Eng.*, Thessaloniki, Greece.

ASTM D7400 / D7400M - 19. 2019. *Standard Test Methods for Downhole Seismic Testing*.

Atkinson G.M. and Boore D.M. 2003. Empirical ground-motion relations for subduction zone earthquakes and their application to Cascadia and other regions: *Bulletin of the Seismological Society of America*, 93 (4), 1703–1729.

Atkinson G. and Boore D. 2006. Earthquake Ground-Motion Prediction Equations for Eastern North America, *Bulletin of the Seismological Society of America*, 96 (6), 2181-2205.

Atkinson G. 2008. Ground-Motion Prediction Equations for Eastern North America from a Referenced Empirical Approach: Implications for Epistemic Uncertainty, *Bulletin of the Seismological Society of America*, 98 (3), 1304-1318.

Atkinson G.M. and Boore D.M. 2008. Erratum to Empirical Ground-Motion Relations for Subduction-Zone Earthquakes and their Application to Cascadia and Other Regions, *Bulletin of the Seismological Society of America*, 98 (5), 2567-2569.

Atkinson G.M. and Boore D.M. 2011. Modifications to Existing Ground-Motion prediction Equations in Light of New Data, *Bulletin of the Seismological Society of America*, 101 (3), 1121-1135.

Boore D.M., Stewart J.P., Seyhan E. and Atkinson G.M. 2014. NGA-West 2 Equations for Predicting PGA, PGV, and 5%-Damped PSA for Shallow Crustal Earthquakes, *Earthquake Spectra* 30 (3), 1057-1085.

Boulanger R.W. and Idriss, I.M. 2014. *CPT and SPT based Liquefaction Triggering Procedures*, Report No UCD/CGM-14/01, Center for Geotechnical Modeling, Department of Civil and Environmental Engineering, University of California, Davis, California, April.

Campbell K.W. and Bozorgnia Y. 2014. NGA-West2 Ground Motion Model for the Average Horizontal Components of PGA, PGV, and 5% Damped Linear Acceleration Response Spectra, *Earthquake Spectra*, 30 (3), 1087-1115.

Chiou B.S.J. and Youngs R.R. 2014. Update of the Chiou and Youngs NGA Model for the Average Horizontal Component of Peak Ground Motion and Response Spectra, *Earthquake Spectra*, 30 (3), 1117-1153.

Darendeli M. 2001. *Development of a new family of normalized modulus reduction and material damping curves*, Ph.D. Thesis, Dept. of Civil Eng., Univ. of Texas, Austin.

Groholski D.R., Hashash Y.M.A, Musgrove M., Harmon J. and Kim B., 2015. Evaluation of 1-D Non-linear Site Response Analysis using a General Quadratic/Hyperbolic Strength-Controlled Constitutive Model, *6th International Conference on Earthquake Geotechnical Engineering*, 1-4 November, Christchurch, New Zealand.

Hashash Y.M.A, Groholski D.R., Phillips C. A., Park D. and Musgrove M. 2015. *DEEPSOIL 6.1, User Manual and Tutorial*.

Idriss I. M. and Boulanger R. W. 2008. *Soil Liquefaction During Earthquakes*, Earthquake Engineering Research Institute.

Jamali F., Aghda S.M.F. and Aliyari A. 2006. Evaluation of seismic sources for hazard assessment in the Fujairah Emirate (UAE), *International Association of Engineering Geologists 10th International Congress*, Nottingham, U.K., paper number 305, p. 6.

Mayne P.W. 2006. In situ test calibrations for evaluating soil parameters, *Proc., Characterization and Engineering Properties of Natural Soils II*, Singapore.

Pezeshk S., Zandieh A. and Tavakoli B. 2011. Hubrid Empirical Ground-Motion Prediction Equations for Eastern North America Using NGA Models and Updated Seismological Parameters, *Bulletin of the Seismological Society of America*, 101 (4), 1859-1870.

Robertson P.K. 1990. Soil classification using the cone penetration test, *Canadian Geotechnical Journal* 27 (1), 151-158.

Robertson P.K. 2009. Interpretation of cone penetration tests – a unified approach, *Canadian Geotechnical Journal* 46 (11), 1337–1355.

Shabani E. and Mirzaei N. 2007. Probabilistic Seismic Hazard Assessment of the Kermanshah-Sanandaj Region of Western Iran, *Earthquake Spectra* 23 (1), 175-197.

Shedlock K. M., Giardini D., Grünthal G. and Zhang P. 2000. The GSHAP Global Seismic Hazard Map, *Seismological Research Letters* 71 (6), 679-686.

Silva W., Gregor N. and Darragh R. 2002. *Development of regional hard rock attenuation relationships for central and eastern North America*, Pacific Engineering and Analysis, 311 Pomona Ave., El Cerrito, CA 94530, 57 p.

Tavakoli B. and Ghafory-Ashtiany M. 2004. *Seismic Hazard Assessment of Iran*, International Institute of Earthquake Engineering and Seismology, Global Seismic Hazard Analysis Project, p. 11.

Thenhaus P.C., Algermissen S.T., Perkins D.M., Hanson S.L. and Diment W.H. 1989. *Probabilistic estimates of the seismic ground-motion hazard in western Saudi Arabia*, U.S. Geological Survey Bulletin 1868.

Thomas P. Wong I. and Abrahamson N. 2010. *Verification of Probabilistic Seismic Hazard Analysis Computer Programs*, Pacific Earthquake Engineering Research Center, PEER Report 2010/106, College of Engineering, University of California, Berkeley, May.

Toro G.R. Abrahamson N.A. and Schneider J.F. 1997. Model for Strong Ground Motions from Earthquakes in Central and Eastern North America: Best Estimates and Uncertainties, *Seismological Research Letters* 68 (1), 41-57.

Wyss M. and Al-Homoud A. 2004. Scenarios of Seismic Risk in the United Arab Emirates, an Approximate Estimate, *Natural Hazards* 32, 375-393.

Youd T.L., Idriss I.M., Andrus R.D., Arango I., Castro G., Christian J.T., Dobry R., Finn W.D.L., Harder Jr L.F., Hynes M.E., Ishihara K., Koester J.P., Liao S.S.C., Marcuson III W.F., Martin G.R., Mitchell J.K., Moriwaki Y., Power M.S., Robertson P.K., Seed R.B. and Stokoe II K.H. 2001. Liquefaction Resistance of Soils: Summary Report from the 1996 NCEER and 1998 NCEER/NSF Workshops on Evaluation of Liquefaction Resistance of Soils, *Journal of Geotechnical and Geoenvironmental Engineering* 127 (10), 817-833.

Youngs R.R. and Coppersmith K.J. 1985. Implications of fault slip rates and earthquake recurrence models to probabilistic seismic hazard estimates, *Bulletin of the Seismological Society of America*, 75 (4), 939-964.

Zhao J.X., Zhang J., Asano A., Ohno Y., Oouchi T., Takahashi T., Ogawa H., Irikura K., Thio H., Somerville P., Fukushima Y. and Fukushima, Y. 2006. Attenuation relations of strong ground motion in Japan using site classification based on predominant period: Bulletin of the Seismological Society of America 96 (3), 898–913.